Original Article

Value of 3.0T magnetic resonance imaging in the diagnosis of retroperitoneal tumors

Zheng Zhu[#], Yanfeng Zhao[#], Xin-Ming Zhao, Xiaoyi Wang, Jingrui Dai, Han Ouyang, Chunwu Zhou

Department of Diagnostic Radiology, National Cancer Center/National Clinical Research Center for Cancer/Cancer Hospital, Chinese Academy of Medical Sciences and Peking Union Medical College, Beijing 100021, China

Contributions: (I) Conception and design: J Dai, XM Zhao; (II) Administrative support: XM Zhao, H Ouyang, C Zhou; (III) Provision of study materials or patients: Z Zhu, Y Zhao; (IV) Collection and assembly of data: Z Zhu, Y Zhao; (V) Data analysis and interpretation: Z Zhu, J Dai; (VI) Manuscript writing: All authors; (VII) Final approval of manuscript: All authors.

[#]These authors contributed equally to this work.

Correspondence to: Xin-Ming Zhao. Department of Diagnostic Radiology, National Cancer Center/National Clinical Research Center for Cancer/Cancer Hospital, Chinese Academy of Medical Sciences and Peking Union Medical College, 17, Panjiayuan Nanli, Chaoyang District, Beijing 100021, China. Email: xinmingzh@sina.com.

Background: To evaluate the diagnostic value of 3.0T MR for differentiating benign from malignant primary retroperitoneal tumors (RPTs).

Methods: A total of 81 patients (44 males and 37 females; 31 benign and 50 malignant lesions) who underwent surgical resection for RPT were evaluated retrospectively. The MR features included lesion location, number, size, margin, surfaces, texture (solid or non-solid), $MR_{hyperintense}$ and $MR_{hypointense}$ signal intensity, apparent diffusion coefficient (ADC) value and the presence of fat, necrosis and hemorrhage. Categorical variables were tested with a χ^2 test or Fisher's exact test for the diagnostic indices and the sensitivity and specificity of MR characteristics.

Results: Using six indices (ill-defined margins, irregular surface, major diameter >5.85 cm, minor diameter >5.35 cm, solid texture and ADC $<1.2\times10^{-3}$ mm^2/s) to diagnose malignant RPT, sensitivity and specificity were 36.0% *vs.* 93.5%, 68.0% *vs.* 58.1%, 80.0% *vs.* 64.5%, 64.0% *vs.* 90.3%, 65.0% *vs.* 63.5%, and 64.0% *vs.* 74.2%, respectively. Combining all those radiological features into a comprehensive evaluation, sensitivity and specificity were 82.0% and 77.4%, respectively (χ^2=27.984, P<0.001) when scores ≥4. Other findings had no statistical significance.

Conclusions: More accurate differential diagnosis of primary RPTs could be made through comprehensive analysis of combined diagnostic indices.

Keywords: Retroperitoneal tumor (RPT); magnetic resonance imaging (MRI); apparent diffusion coefficient value

Submitted Nov 17, 2018. Accepted for publication May 14, 2019.
doi: 10.21037/tcr.2019.05.16
View this article at: http://dx.doi.org/10.21037/tcr.2019.05.16

Introduction

Retroperitoneal tumors (RPTs) arise from within the retroperitoneal cavity (1), but external to the retroperitoneal organs. Various types of tumors can arise in the retroperitoneal space, and may be classified as cystic or non-cystic lesions (2) and fat-containing or fat-deficient (3), with a majority being mesenchymal, neurogenic, embryonic urogenital, or lymphatic system tumors.

The optimal treatment approach for RPTs is surgical removal (4-7) when they are localized with no evidence of distant metastasis. Despite surgical removal, local recurrence is the primary mode of failure in up to 50% of the cases at five years post-surgery (8-11). Thus, accurate

Table 1 Scan parameter of MR scan

Scan parameter	AxiFSE T1WI in-phase	T1WI out-phase	Axi FRFSE-T2	Axi FSE T2/FS	DWI	Axi LAVA+C	Cor LAVA+C	Sag LAVA+C
TE (ms)	2.3	5.8	85–107	89–107	50–65	1.3–1.9	1.6–1.8	1.6–1.8
TR (ms)	255–285	255–285	4,500–7,500	6,600–7,500	4,500–5,100	2.7–3.9	3.7–4.2	3.7–4.2
FOV	35×35	35×35	35×35	35×35	35×35	35×35	40×40	40×40
FLIP	80	80	80–90	80–90	80–90	12–15	12–15	12–15
NEX	0.75	0.75	2	2	2	0.75	0.75	0.75
ASSET	2.0	2.0	2.0	2.0	2.0	2.0	2.0	2.0
Thickness (mm)	7.0	7.0	6–7	6–7	7.0	4.5–5.0	4.5–5.0	4.5–5.0
Layer spacing (mm)	1.0	1.0	1.0	1.0	1.0	0	0	0
ETL	1	1	12–17	12–17	1	1	1	1
Matrix	288×192	288×192	288×224	288×224	128×128	288×180	288×192	288×180
Gate	–	–	+	+	–	–	–	–
Hold breath	+	+	–	–	+	+	+	+

+, with; –, without. TE, echo time; TR, reputation time; FOV, field of view; NEX, number of excitation; ASSET, array spatial sensitivity encoding technique; ETL, echo train length.

preoperative localization and characterization of RPTs is important for allowing a direct surgical approach. Although most RPTs present with similar clinical findings and their diagnosis is often challenging for radiologists, predominant or specific features are present in the various types, and have a tendency to occur in uncommon places (12-15). Findings on functional magnetic resonance imaging (MRI) have been reported to have the potential to differentiate pathologically malignant tumors from the benign types (16). However, the radiographic features of retroperitoneal neoplasms often overlap. Single, nonspecific image features are insufficient for the differentiation of tumor type.

To our knowledge, there have been few studies that have addressed the statistical correlation between MRI findings and the differentiation between benign and malignant tumors of RPT. Therefore, in this study, we aim to differentiate between benign and malignant tumors using malignant scores.

Methods

Patients and clinical data

The Institutional Review Board (IRB) of our hospital waived the need for approval and ruled out the need for obtaining informed consent from the patients. All information obtained from patients was anonymized and de-identified prior to analysis. Between January 2011 and January 2017, 103 patients with a diagnosis of RPT were retrospectively identified at our hospital. Among these patients, 22 were excluded from the study either because a preoperative MRI examination had not been performed (n=18) or because the patient did not undergo surgical treatment (n=4). The remaining 81 patients (44 males and 37 females) with a median age of 52 years (range, 12–79 years) were enrolled in this study. The full clinical records of those patients were reviewed retrospectively. Contrast-enhanced MRI was performed in 67 patients (82.7%), while non-enhanced MRI was performed in 14 (17.3%) due to patients' allergy to the contrast material or unwillingness to undergo contrast enhanced MRI.

MRI scans

MRI was performed in all 81 patients using a 3.0T MR superconductivity scanner (Signa Excite, GE Healthcare, USA). The scan parameters were shown in *Table 1*.

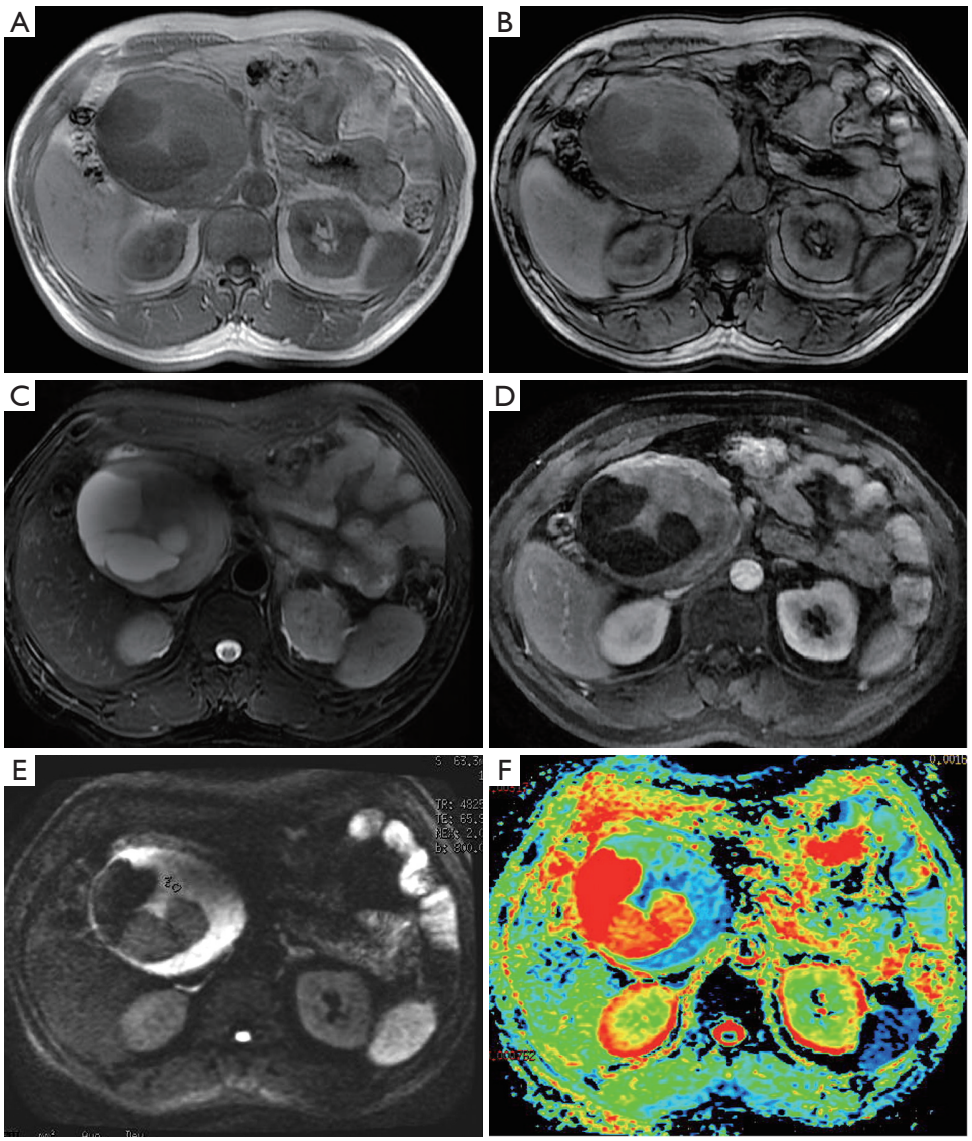

Figure 1 A female who is 52 years old. The mass was found on check-up for one month. The tumor had regular shape and well-defined margin, showed hypointense on T1WI/DUAL (A/B), heterogeneous hyperintense on T2WI/FS (C), and marked enhanced on enhanced MR imaging (D). And hyperintense on DWI (E). ADC =2.117×10^{-3} mm^2/s (F). Pathology: neurofibroma.

Image analysis

The MRI scans were reviewed by two radiologists (with 29 and 14 years of experience, respectively) who were unaware of the histopathologic diagnoses, but had knowledge of the clinical data. Final consensus was reached for: (I) lesion location (17); (II) number of lesions (single or multiple); (III) lesion size (major diameter and minor diameter); (IV) lesion margins (well defined or ill-defined); (V) morphology [oval/round or others (irregular)]; (VI) T1/T2 signal intensity (homogeneous or heterogeneous); (VII) MRI values for high and low signal intensity [well contrast enhanced or poorly contrast enhanced tumor signal intensity in the portal-venous phase was measured by manually placing regions of interest (ROI) in the hyperintense or hypointense area]; and (VIII) tumor apparent diffusion coefficient (ADC) value in mm^2/s was measured by placing ROI which were round, 30–50 mm^2 square and consisted of more than 20 pixels in the lowest ADC values area of solid part of the tumor (*Figure 1*). In addition, the radiologists were asked

to document the presence of septae, hemorrhage, necrosis, and fat.

Statistical analysis

The sensitivity, specificity, and accuracy of the diagnostic criteria were used to describe the morphology of the lesion. The counting data were expressed by rate using the Chi squared test (Pearson or McNemar), and the quantitative data were compared using the *t*-test and F test. Receiver operating characteristic (ROC) analysis was performed, and the area under the curve (AUC) was calculated. This study evaluated the comprehensive indices with all significant MRI values, each of which was assigned a score if one of the indices applied to each lesion, by combining the various statistically significant indices to calculate the Youden Index (YI) and find the optimal diagnostic threshold score. The sensitivity, specificity, and accuracy of the threshold were calculated, at inspection level α=0.05. When P values using SPSS software, version 18.0 (IBM, NY, USA) were <0.05, the difference was considered statistically significant. The cartogram was drawn by GraphPad Prism software, version 7.0 (GraphPad, CA, USA).

Results

Clinical data

Fifty-three patients (65.4%) were asymptomatic, and the remainder presented with abdominal discomfort (21 cases; 25.9%), backache (5 cases; 6.2%), or fatigue (2 cases; 2.5%). Seventy-six patients (93.8%) had a single lesion while five patients (6.2%) had multiple lesions; 50 cases (61.7%) were malignant, and 31 cases (38.3%) were benign.

Pathological type and retroperitoneal space classification

The pathological types of the tumors are shown in *Table 2*. Based on studies by Tirkes *et al.* (17), Shanbhogue *et al.* (18), and retroperitoneal anatomy (1), the 81 cases were subgrouped into four cross-sectional spaces according to the pathology.

Indicators differentiating benign and malignant RPTs

Lesion margin

Diagnosis of malignant lesions among the RPTs on the basis of ill-defined borders in the MRI scans was found to be statistically significant. Use of an ill-defined border as the criterion for diagnosis of malignant lesions among the RPTs was statistically significant. The sensitivity and specificity were 36.0% and 93.5%, respectively (χ^2=8.98, P=0.003) (*Table 3*). In total, 61 cases (75.3%) had well defined margins, including 29 benign (47.5%) and 32 malignant tumors (52.5%), while 20 cases (24.7%) had ill-defined margins, including 2 benign (10%) and 18 malignant tumors (90%).

Lesion morphology

Use of an irregular shape as the criterion also had statistical significance. The sensitivity and specificity were 68.0% and 58.1%, respectively (χ^2=5.338, P=0.021). In total, 34 cases (42%) including 18 benign and 16 malignant tumors had oval/round shapes, while 47 cases (58%) including 13 benign and 34 malignant tumors had irregular shapes.

Solid or mixed cystic and solid texture of the lesions

Use of a solid texture as the criterion was statistically significant as well (χ^2=5.857, P=0.040). In total, 69 solid lesions (85.2%) included 24 benign (34.8%) and 45 malignant tumors (65.2%), and 12 mixed solid and cystic lesions (13.3%) included 7 benign (58.3%) and 5 malignant tumors (41.7%). A higher solid content in tumors was correlated with malignancy.

Lesion size

Major diameters were 1.5–21.0 cm with mean of 8.2 cm; minor diameters were 1.4–17.1 cm with mean of 6.1 cm (*Figure 2A*). A larger size correlated with malignancy. ROC curves plotted for long and short diameters showed the following: AUC_{major} =0.748, P_{major} <0.001; AUC_{minor} =0.766, P_{minor} <0.001 (*Figure 2B*). The calculated YI indicated that a major diameter >5.85 cm and a minor diameter >5.35 cm were the best diagnostic thresholds for diagnosing malignant lesions among the RPT; the sensitivity and specificity were 80.0% and 64.5%, 64.0% and 90.3%, respectively (χ^2_{major}=16.261, P_{major} <0.001; χ^2_{minor} =23.012, P_{minor} <0.001).

ADC value

The $ADC_{malignant}$ =1.185×10^{-3} mm^2/s [range =(0.525–2.62)×10^{-3} mm^2/s, mean =1.078×10^{-3} mm^2/s] and ADC_{benign} =1.705×10^{-3} mm^2/s [range =(0.688–3.15)×10^{-3} mm^2/s, mean =1.523×10^{-3} mm^2/s] (*Figure 3A*). The difference in ADC between benign and malignant RPT had statistical significance (*t*=3.657, P<0.001) (*Figure 3B*). The best threshold for diagnosing malignant RPT was 1.2×10^{-3} mm^2/s;

Table 2 Pathological types of the 81 RPT cases

Pathological type	Patients (%)	Males (%)	Females (%)	Median age (years)	Number of patients with comprehensive evaluation index ≥4 (%)
Neurogenic tumors	32 (39.5)	19 (59.4)	13 (40.6)	50	9 (28.1)
Paraganglioma	17 (21.0)	11 (64.7)	6 (35.3)	45	4 (23.5)
Schwannoma	10 (12.3)	6 (60.0)	4 (40.0)	51	3 (30.0)
Ganglioneuroma	3 (3.7)	1 (33.3)	2 (66.7)	52	2 (66.7)
Neurofibroma	1 (1.2)	1 (100.0)	0	–	0
Neuroendocrine tumors	1 (1.2)	0	1 (100.0)	–	0
Mensenchymal tumors	46 (56.8)	24 (52.2)	22 (47.8)	53	40 (87.0)
Liposarcoma	24 (29.6)	13 (54.2)	11 (45.8)	53	21 (87.5)
Sarcoma	4 (4.9)	1 (25.0)	3 (75.0)	58	4 (100.0)
Spindle cell sarcoma	4 (4.9)	2 (50.0)	2 (50.0)	51	4 (100.0)
MFH	4 (4.9)	2 (50.0)	2 (50.0)	58	2 (50.0)
Fibrosarcoma	3 (3.7)	2 (66.7)	1 (33.3)	36	3 (100.0)
Lipoma	1 (1.2)	0	1 (100.0)	–	1 (100.0)
Rhabdomyosarcoma	1 (1.2)	1 (100.0)	0	–	0
Sclerosing fibromatosis	1 (1.2)	1 (100.0)	0	–	1 (100.0)
Sarcoma (unclassified)	4 (4.9)	2 (50.0)	2 (50.0)	52	4 (100.0)
Reproductive residual embryo tissue origin	2 (2.5)	1 (50.0)	1 (50.0)	50.5	2 (100.0)
Teratoid tumors	1 (1.2)	0	1 (100.0)	–	1 (100.0)
Seminoma	1 (1.2)	1 (100.0)	0	–	1 (100.0)
Lymphatic hematopoietic system tumors	1 (1.2)	0	1 (100.0)	–	0
Lymphoma	1 (1.2)	0	1 (100.0)	–	0
Total	81 (100.0)	44 (54.3)	37 (45.7)	52	51 (63.0)

MFH, malignant fibrous histosarcmoa; RPT, retroperitoneal tumor.

Table 3 Indexes that had diagnostic value

Variable	Sensitivity (%)	Specificity (%)	Statistical method	P value
$MR_{ill\text{-}defined}$	36.0	93.5	8.98*	0.003
$MR_{irregular}$	68.0	58.1	5.338*	0.021
Solid	65.0	63.5	5.857*	0.040
Long diameter >5.85 cm	80.0	64.5	16.261*	<0.001
Short diameter >5.35 cm	64.0	90.3	23.012*	<0.001
$MR_{hyperintense}$ value	–	–	0.469†	0.685
$MR_{hypointense}$ value	–	–	0.590†	0.240
ADC value	64.0	74.2	0.724†	0.001

*, χ^2-test; †, AUC method.

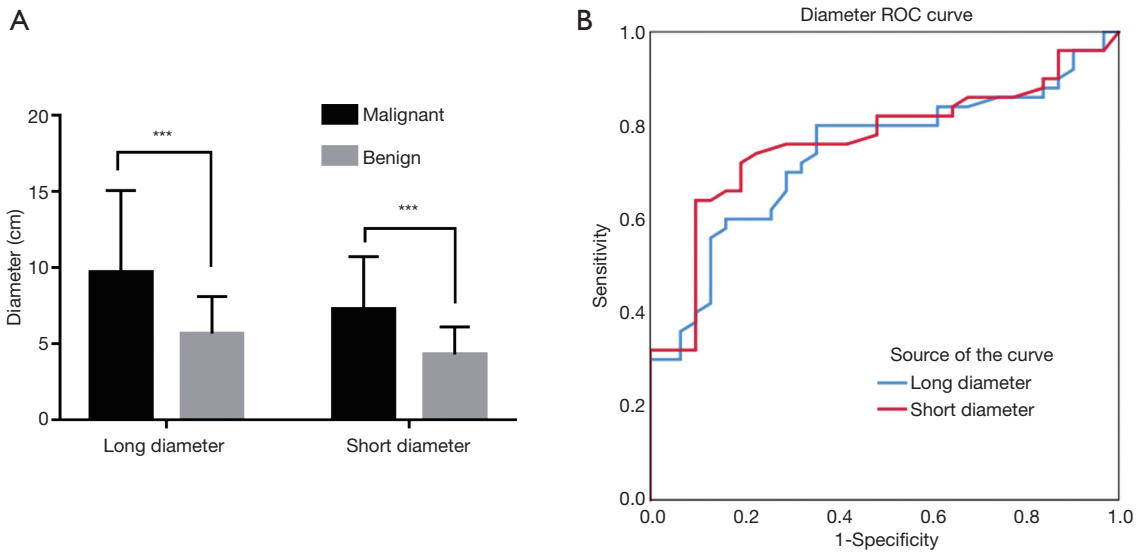

Figure 2 The long and short diameter between benign and malignant retroperitoneal tumors. (A) Showed the bar chart of long and short diameter (***, P<0.001); (B) showed ROC curves of long and short diameter for diagnosing RTs by 3.0T MR. ROC, receiver operating characteristic.

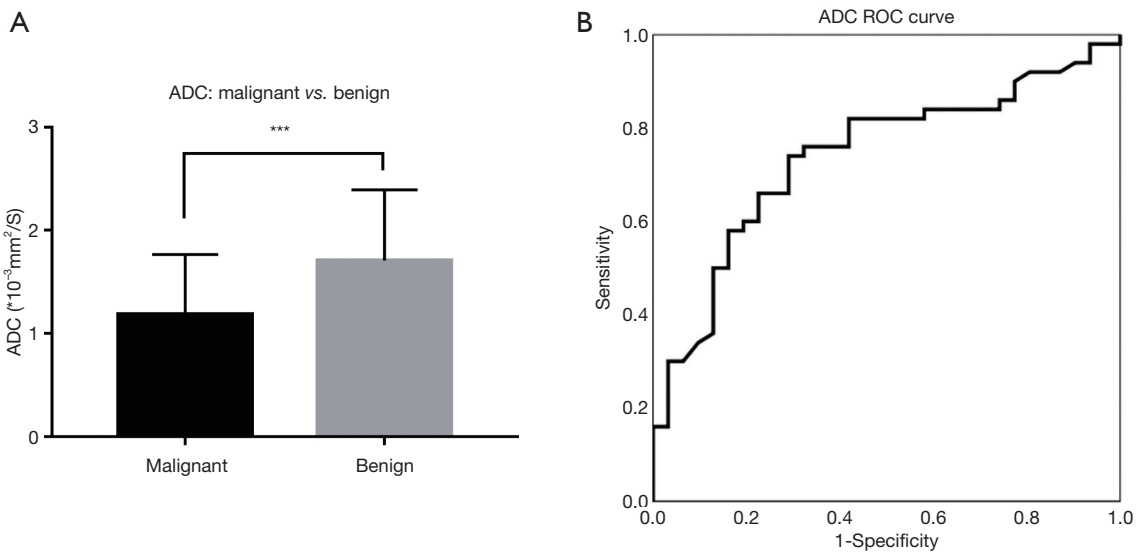

Figure 3 The ADC value between benign and malignant retroperitoneal tumors. (A) Showed the bar chart of ADC value (***, P<0.001); (B) showed ROC curves of ADC value for diagnosing RTs by 3.0T MR. ADC, apparent diffusion coefficient; ROC, receiver operating characteristic.

the sensitivity and specificity were 64% and 74.2%, respectively (χ^2=11.167, P=0.001), accuracy were 61.7%.

Indicators with no statistical significance

The MR signal intensity was also analyzed, the results showed no statistical significance (*Table 4*).

Comprehensive evaluation index

Malignant scores were calculated by combining all six statistically significant diagnostic indices as a multiple

Table 4 The multiple evaluation indexes for diagnosing RPT by 3.0T MR

Variable	Area	Std. error	Asymptotic sig.	Lower bound	Upper bound
Long diameter	0.738	0.055	<0.001	0.630	0.847
Short diameter	0.766	0.053	0.000	0.661	0.871
$MR_{hyperintense}$	0.469	0.075	0.685	0.323	0.615
$MR_{hypointense}$	0.590	0.074	0.240	0.444	0.736
ADC value	0.739	0.056	<0.001	0.630	0.849
Multiple index	0.868	0.041	<0.001	0.787	0.949

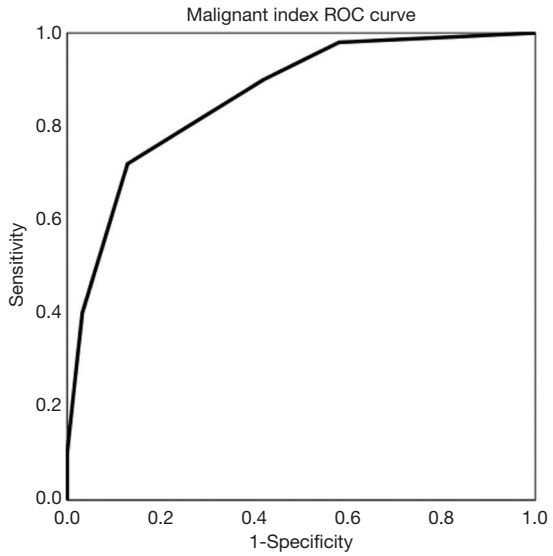

Figure 4 The ROC curves for multiple evaluation indexes for diagnosing RTs by 3.0T MR. ROC, receiver operating characteristic.

evaluation index. In this study, the malignant score was calculated by malignant indices for each tumor. In addition, the total number was calculated and the score curve was plotted. The ROC curve provided the best determination threshold (*Figure 4*). Higher scores were correlated with higher chances of malignancy.

This study evaluated the comprehensive indices with significant MRI values, each of which was assigned a score if one of the indices applied to the lesion (ill-defined border scores 1, well-defined border scores 0; irregular shape scores 1, round or oval shape score 0; solid scores 1, cystic and mixed solid and cystic score 0; major diameter >5.85 cm scores 1, major diameter <5.85 cm scores 0; minor diameter >5.35 cm scores 1, minor diameter <5.35 cm scores 0; and ADC $<1.2\times10^{-3}$ mm^2/s scores 1, ADC $>1.2\times10^{-3}$ mm^2/s scores 0). Based on the malignant score, the present study calculated YI, and demonstrated that a score ≥4 was the best diagnostic threshold (*Table 3*). The sensitivity and specificity for this score was 82.0% and 77.4%, respectively (χ^2=27.984, P<0.001).

Discussion

The retroperitoneal space is deep, and a neoplasm in this area usually presents with no specific symptom except abdominal discomfort or distention. The RPTs have a variable and non-specific presentation and may resemble with other neoplastic lesions. The RPT could be preliminarily diagnosed by location and MRI, providing a reference for clinical treatment. However, there are many pathological types of neoplasms in the retroperitoneal space. Our study included 17 different types of RPTs, without including all pathological types. MRI manifestations of RPT are complex. The various MRI signs demonstrate an intersection between different pathological lesions and benign and malignant lesions. Single signs are not sufficient for the diagnosis of benign and malignant RPT.

Margin, morphology, solidity, major diameter, minor diameter, and ADC value of the lesion are the six indicators that could predict the malignant nature of the RPT. Margin and morphology are usually indicators that help to differentiate benign from malignant tumors. Ill-defined border and irregular shape were used to indicate malignancy in our study. Demehri *et al.* (19) also reported that ill-defined or infiltrative margins are factors that can predict malignancy. Solid lesions had high tendency toward malignancy than cystic or mixed solid and cystic lesions in our study. The most common cystic lesions in the retroperitoneal space are lymphangioma and cystic mesothelioma, and most of them are usually benign (20). In terms of size, our study showed that a bigger size correlated with greater tendency for malignancy. Major diameter

>5.85 cm or minor diameter >5.35 cm can be used as the diagnostic indicators to indicate malignancy. Demehri *et al.* (19) also reported that a bigger size of the tumor with ill-defined or infiltrative margins, peritumoral edema, and early arterial enhancement are factors that can predict malignancy. However, all malignant peripheral nerve sheath tumors occurred in patients with neurofibromatosis. Our study did not take early arterial enhancement into consideration. Instead, we used the MRI signal intensity which showed no statistical significance in the differentiation of benign from malignant RPT. With regard to the ADC value, Nagata *et al.* (21) shared the opinion that the mean ADC value of benign non-myxoid tumors [$(1.31\pm0.46)\times10^{-3}$ mm^2/s] was significantly higher than that of malignant non-myxoid tumors [$(0.94\pm0.25)\times10^{-3}$ mm^2/s] ($P<0.001$). In their report on diffusion weighted imaging of peripheral nerve sheath tumors throughout the body, Demehri *et al.* (19) reported that only minimum ADC was useful. However, contrary to this, Chhabra *et al.* (16) reported that minimum ADC was not useful.

The purpose of our study was to convert subjective analyses of radiologists into a more objective evaluation, which increased their statistical value. We found that six evaluation indices had statistical value, by combining the various statistically significant indices to calculate the YI. We found that a total score ≥4 was the best diagnostic threshold from which a meaningful radiological result could be declared. However, we have to admit that the sensitivity and specificity obtained by malignant score indices do not seem to be superior to the sensitivity and specificity of the single factor. In other words, using a single factor in the clinical patients might have a time advantage over the malignant score.

Our study has several limitations. First, it was limited by its retrospective nature. Second, our study incorporated six findings which were obtained by the univariate analysis into malignant score indices. All six factors may not necessarily be independent predictive factors of malignancy. However, this has been ignored in many medical journals. We could use a multivariate analysis, such as logistic regression model, when enrolling more patients in the near future. And more importantly, we only differentiated the benign RPT from the malignant through the MRI, and did not focus on texture analysis or radiomics of the images. Kim *et al.* (22) reported that texture analysis of the ADC could be useful for the diagnosis of malignancy of myxoid tissue such as in schwannoma. Finally, we only mentioned the diagnosis, but did not provide the prognosis of the different treatments for RPT. Nussbaum and colleagues (23) found that both preoperative and postoperative radiotherapy were significantly independent predictors of improved overall survival in retroperitoneal sarcoma.

In summary, RPTs represent a diverse group of neoplasms, often with non-specific imaging findings. The MRI manifestations of benign and malignant lesions and different pathological types of the lesions usually overlap. It is difficult to obtain a better diagnosis no matter what indicator is used alone. A more accurate and stable diagnosis could be made through a comprehensive analysis of the various meaningful diagnostic indicators and signs of RPT.

Acknowledgments

Funding: None.

Footnote

Conflicts of Interest: All authors have completed the ICMJE uniform disclosure form (available at http://dx.doi.org/10.21037/tcr.2019.05.16). The authors have no conflicts of interest to declare.

Ethical Statement: The authors are accountable for all aspects of the work in ensuring that questions related to the accuracy or integrity of any part of the work are appropriately investigated and resolved. The study was conducted in accordance with the Declaration of Helsinki (as revised in 2013). The Institutional Review Board (IRB) of our hospital waived the need for approval and ruled out the need for obtaining informed consent from the patients.

References

1. Coffin A, Boulay-Coletta I, Sebbag-Sfez D, et al. Radioanatomy of the retroperitoneal space. Diagn Interv

Imaging 2015;96:171-86.
2. Rajiah P, Sinha R, Cuevas C, et al. Imaging of uncommon retroperitoneal masses. Radiographics 2011;31:949-76.
3. Craig WD, Fanburg-Smith JC, Henry LR, et al. Fat-containing lesions of the retroperitoneum: radiologic-pathologic correlation. Radiographics 2009;29:261-90.
4. Giuliano K, Nagarajan N, Canner JK, et al. Predictors of improved survival for patients with retroperitoneal sarcoma. Surgery 2016;160:1628-35.
5. Okuyama T, Tagaya N, Saito K, et al. Laparoscopic resection of a retroperitoneal pelvic schwannoma. J Surg Case Rep 2014;2014.
6. Maurice MJ, Yih JM, Ammori JB, et al. Predictors of surgical quality for retroperitoneal sarcoma: Volume matters. J Surg Oncol 2017;116:766-74.
7. Kuriakose S, Vikram S, Salih S, et al. Unique surgical issues in the management of a giant retroperitoneal schwannoma and brief review of literature. Case Rep Med 2014;2014:781347.
8. Stahl JM, Corso CD, Park HS, et al. The effect of microscopic margin status on survival in adult retroperitoneal soft tissue sarcomas. Eur J Surg Oncol 2017;43:168-74.
9. Gronchi A, Strauss DC, Miceli R, et al. Variability in Patterns of Recurrence After Resection of Primary Retroperitoneal Sarcoma (RPS): A Report on 1007 Patients From the Multi-institutional Collaborative RPS Working Group. Ann Surg 2016;263:1002-9.
10. Toulmonde M, Bonvalot S, Meeus P, et al. Retroperitoneal sarcomas: patterns of care at diagnosis, prognostic factors and focus on main histological subtypes: a multicenter analysis of the French Sarcoma Group. Ann Oncol 2014;25:735-42.
11. Leiting JL, Bergquist JR, Hernandez MC, et al. Radiation Therapy for Retroperitoneal Sarcomas: Influences of Histology, Grade, and Size. Sarcoma 2018;2018:7972389.
12. Harada TL, Nagao G, Aoyagi T, et al. Giant retroperitoneal schwannoma in a 52-year-old man. Radiol Case Rep 2018;13:810-4.
13. Lee EJ, Song KJ, Seo YS, et al. A solitary malignant schwannoma in the choana and nasal septum. Case Rep Otolaryngol 2014;2014:202910.
14. Xu H, Sha N, Li HW, et al. A giant pelvic malignant schwannoma: a case report and literature review. Int J Clin Exp Pathol 2015;8:15363-8.
15. Scali EP, Chandler TM, Heffernan EJ, et al. Primary retroperitoneal masses: what is the differential diagnosis? Abdom Imaging 2015;40:1887-903.
16. Chhabra A, Thakkar RS, Andreisek G, et al. Anatomic MR imaging and functional diffusion tensor imaging of peripheral nerve tumors and tumorlike conditions. AJNR Am J Neuroradiol 2013;34:802-7.
17. Tirkes T, Sandrasegaran K, Patel AA, et al. Peritoneal and retroperitoneal anatomy and its relevance for cross-sectional imaging. Radiographics 2012;32:437-51.
18. Shanbhogue AK, Fasih N, Macdonald DB, et al. Uncommon primary pelvic retroperitoneal masses in adults: a pattern-based imaging approach. Radiographics 2012;32:795-817.
19. Demehri S, Belzberg A, Blakeley J, et al. Conventional and functional MR imaging of peripheral nerve sheath tumors: initial experience. AJNR Am J Neuroradiol 2014;35:1615-20.
20. Mota MMDS, Bezerra ROF, Garcia MRT. Practical approach to primary retroperitoneal masses in adults. Radiol Bras 2018;51:391-400.
21. Nagata S, Nishimura H, Uchida M, et al. Diffusion-weighted imaging of soft tissue tumors: usefulness of the apparent diffusion coefficient for differential diagnosis. Radiat Med 2008;26:287-95.
22. Kim HS, Kim JH, Yoon YC, et al. Tumor spatial heterogeneity in myxoid-containing soft tissue using texture analysis of diffusion-weighted MRI. PLoS One 2017;12:e0181339.
23. Nussbaum DP, Rushing CN, Lane WO, et al. Preoperative or postoperative radiotherapy versus surgery alone for retroperitoneal sarcoma: a case-control, propensity score-matched analysis of a nationwide clinical oncology database. Lancet Oncol 2016;17:966-75.

Cite this article as: Zhu Z, Zhao Y, Zhao XM, Wang X, Dai J, Ouyang H, Zhou C. Value of 3.0T magnetic resonance imaging in the diagnosis of retroperitoneal tumors. Transl Cancer Res 2019;8(3):867-875. doi: 10.21037/tcr.2019.05.16

